HIGH-TEMPERATURE VISCOSITY OF COMMERCIAL GLASSES

PAVEL HRMA

Pacific Northwest National Laboratory, Richland, WA 99352, United States of America

E-mail: pavel.hrma@pnl.gov

Submitted November 11, 2005; accepted December 12, 2005

Keywords: Viscosity, Glass, Viscosity model

Arrhenius models were developed for glass viscosity within the processing temperature range for six types of commercial glasses: low-expansion-borosilicate glasses, E glasses, fiberglass wool, TV panel glasses, container glasses, and float glasses. Both local models (for each of the six glass types) and a global model (for the composition region of commercial glasses, i.e., the six glass types taken together) are presented. The models are based on viscosity data previously obtained with rotating spindle viscometers within the temperature range between 900°C and 1550°C; the viscosity varied from 1 Pas to 750 Pas. First-order models were applied to relate Arrhenius coefficients to the mass fractions of 15 components: SiO_2, TiO_2, ZrO_2, Al_2O_3, Fe_2O_3, B_2O_3, MgO, CaO, SrO, BaO, PbO, ZnO, Li_2O, Na_2O, and K_2O. The R^2 is 0.98 for the global model and ranges from 0.97 to 0.99 for the six local models. The models are recommended for glasses containing 42 to 84 mass% SiO_2 to estimate viscosities or temperatures at a constant viscosity for melts within both the temperature range from 1100°C to 1550°C and viscosity range from 5 to 400 Pas.

INTRODUCTION

The melting behavior of glasses depends on their viscosity-temperature relationships. Glassmelting furnace design and operation are largely determined by the temperature span within which melt viscosity allows successful melting, fining, and conditioning of the glass. Therefore, the knowledge of glass viscosity as a function of temperature and glass composition is crucial for efficient glassmaking.

The most commonly used viscosity-temperature relationship for a wide span of viscosities (over 12 orders of magnitude) is the Vogel-Fulcher-Tammann (VTF) equation,

$$\ln\eta = F_1 + \frac{F_2}{T - T_0} \tag{1}$$

where η is the viscosity, T is the absolute temperature, and F_1, F_2, and T_0 are temperature-independent coefficients [1]. However, during the melting process, the viscosity of molten glass spans only 3 orders of magnitude (1 to 10^3 Pas). For this relatively narrow range, the viscosity-temperature relationship is sufficiently well represented by the Arrhenius equation [2,3],

$$\ln\eta = A + \frac{B}{T} \tag{2}$$

The Arrhenius coefficients, A and B, are functions of glass composition. Since all mixture properties, extensive and non-extensive, are expressible in terms of their partial specific (per mass) or molar values [4], Arrhenius coefficients for viscosity can be related to glass composition as

$$A = \sum_{i=1}^{N} A_i x_i \tag{3}$$

and

$$B = \sum_{i=1}^{N} B_i x_i \tag{4}$$

where A_i and B_i are the i-th component partial specific Arrhenius coefficients, and N is the total number of components.

The A_i and B_i values are relatively constant within the range of composition of commercial glasses. Therefore, equations (3) and (4) can be treated as linear models and A_i and B_i as component coefficients for glass viscosity. We can also introduce the i-th component partial specific viscosity, i.e., a temperature-dependent coefficient, defined as

$$\eta_i = \exp\left(A_i + \frac{B_i}{T}\right) \tag{5}$$

Based on the partial specific values (component coefficients), the viscosity of molten glass (within the glass melting temperature range) can be estimated using the equation

$$\eta = \exp\left(\sum_{i=1}^{N}\left[A_i + \frac{B_i}{T}\right]x_i\right) \tag{6}$$

or

$$\ln \eta = \sum_{i=1}^{N} x_i \ln \eta_i \tag{7}$$

which can also be written as

$$\eta = \prod_{i=1}^{N} \eta_i^{x_i} \tag{8}$$

A convenient feature of the Arrhenius equation is its linearity, which allows us to express explicitly the temperature at which viscosity has a desired value. Rearranging equation (6), we obtain

$$T = \frac{\sum_{i=1}^{N} B_i x_i}{\ln \eta - \sum_{i=1}^{N} A_i x_i} \tag{9}$$

To develop mathematical models that represent the viscosity-temperature-composition relationships for commercial glasses, several steps need to be taken [5]. Roughly, the composition and temperature regions must be defined and covered with a matrix of a sufficient number of points. Glasses of the corresponding compositions are then made and tested at several temperatures to generate a database to which equation (6) can be fitted.

Table 1 lists composition regions of six types of commercial glasses evaluated in this study: E-glass (E), float glass (F), low-expansion-borosilicate glass (LE), TV panel glass (TV), fiberglass wool (FW), and container glass (C). The composition matrices of glasses that cover these six regions are presented in [6]. Figure 1 displays the maximum mass fractions of glass components for the overall composition region of commercial glasses tested (the minimum fractions of all components but SiO_2 were 0). As table 1 shows, the SiO_2 mass fraction range is 0.42 to 0.84, and the maximum mass frac-

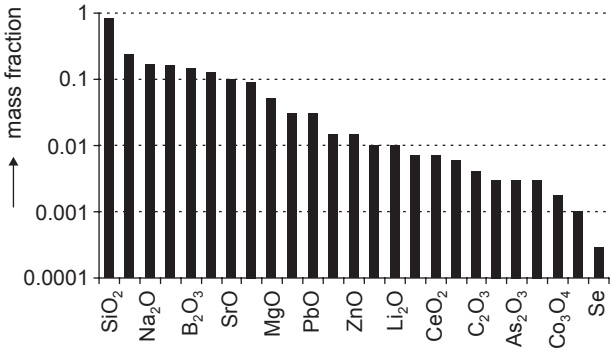

Figure 1. Maximum mass fractions of components in the composition region of commercial glasses .

Table 1. Composition regions of glasses in mass %.

	E	F	LE	TV	FW	C	All
SiO_2	41.6-71.5	67.5-77.3	63-84	50-83	48.6-78	62.5-81	41.6-84
B_2O_3	0-9		10-15		3-9		0-15
Al_2O_3	12-16	0.1-2	2-7	1.3-3.5	0-6	1-3	0-16
MgO	0.5-4.5	3-4		0-1.5	1-5	0-3	0-5
CaO	16-24	7-9	0-2	0-3.5	5-11	7-12	0-24
Na_2O	0-2	12-15	4-8	6-9	13-17	11-15	0-17
K_2O	0-0.5	0-2	0-3	6-9	0-2	0-2	0-9
Fe_2O_3	0-0.8	0.1-1.5			0-0.6	0-0.4	0-1.5
TiO_2	0-1	0-1		0.1-0.5		0-0.5	0-1
F	0-0.6			0-0.7	0-0.6		0-0.7
SO_3					0-0.2	0-0.3	0-0.3
Li_2O				0-0.5		0-1	0-1
Cr_2O_3		0-0.4				0-0.3	0-0.4
BaO			0-2	2-13		0-0.1	0-13
CeO_2				0-0.7			0-0.7
ZrO_2				0-3			0-3
PbO				0-3			0-3
ZnO				0-1.5			0-1.5
As_2O_3				0-0.3			0-0.3
Sb_2O_3				0.2-0.6			0-0.6
SrO				1-10			0-10
MnO_2		0-0.3					0-0.3
Se		0-0.03					0-0.03
Co_3O_4		0-0.2					0-0.2
FeO	0-0.1				0-0.1		0-0.1

E - E glass, F - float glass, LE - low-expansion-borosilicate glass, TV - TV panel glass, FW-fiberglass wool, C - container glass

tions of major components are CaO 0.24, Na_2O 0.17, Al_2O_3 0.16, B_2O_3 0.15, BaO 0.13, SrO 0.10, K_2O 0.09, and MgO 0.05.

Out of the total number of 150 different compositions (25 compositions-baseline plus 24 variations-for each of the six groups), 147 were fabricated at Alfred University and tested in Pacific Northwest National Laboratory (PNNL) where viscosity was measured with rotating spindle viscometers. Hrma et al., Chapter 7 in [6], describe the details of measurement and list the measured viscosity data. Figure 2 maps the viscosity-temperature data points. Note that LE and E glasses occupy the high–viscosity–high–temperature corner, F glasses have relatively small viscosity variations, and FW glasses cover the largest viscosity-temperature area. Overall, the temperature of measurements spanned an interval from 899°C to 1554°C, and the viscosity varied from 1 Pas to 747 Pas.

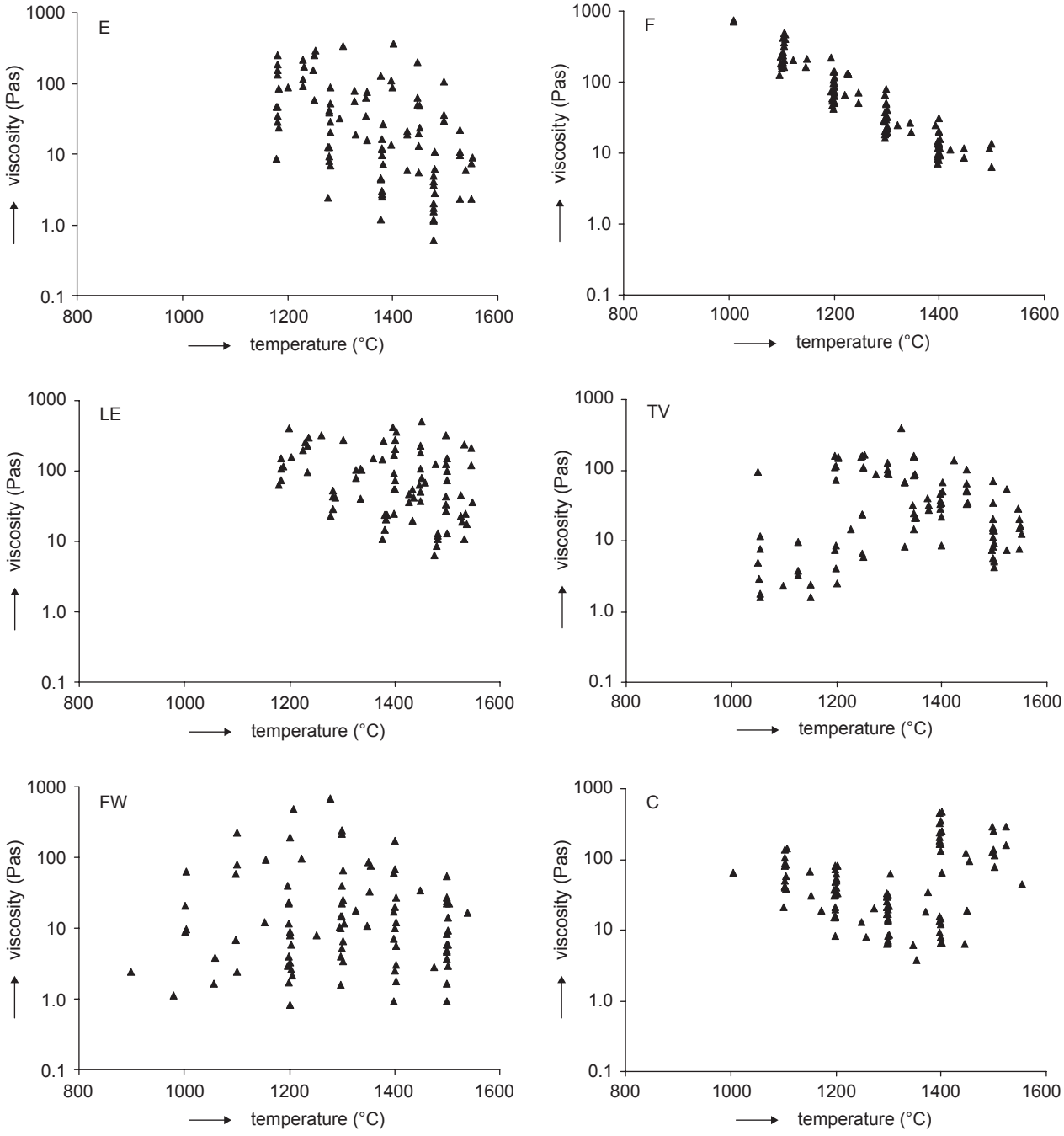

Figure 2. Maps of viscosity-temperature data points for six types of commercial glasses: E glass (E), float glass (F), low-expansion-borosilicate glass (LE), TV panel glass (TV), fiberglass wool (FW), and container glass (C).

Fluegel et al. [7] augmented these low-viscosity data by high-viscosity data measured with the beam bending and parallel plate methods [6] and by published viscosities of an additional 150 glasses. They used the resulting large database to obtain component coefficients for isokoms, i.e., temperatures at constant viscosity (T_η) using the formula

$$T_\eta = T_0 + 10^2 \sum_i T_i c_i + 10^4 \sum_{i,j} T_{ij} c_i c_j + 10^6 \sum_{i,j,k} T_{ijk} c_i c_j c_k \quad (10)$$

where T_0, T_i, T_{ij}, and T_{ijk} are composition-independent coefficients, and c_i is the i-th component mole fraction. The composition-independent coefficients are functions of viscosity and are listed in table 2 for three viscosity values corresponding to log(η (Pas)) = 1.5, 6.6, and 12.0.

Fluegel et al., Chapter 9 in [6], provide also four first-order models for log(η (Pas)) = 1.5, 6.6, and 12.0 isokoms for the following five composition regions: F+C (float glasses plus container glasses), E, TV, LE, and FW. They report the significant coefficients and the intercept, corresponding to the equation

$$T_\eta = T_0 + \sum_{i=1}^{S} b_i x_i \quad (11)$$

where b_i is the significant component coefficient, and S is the number of significant components. This equation can be conveniently rearranged into the form

$$T_\eta = \sum_{i=1}^{N} a_i x_i \quad (12)$$

where $a_i = b_i + T_0$ (i=1,…,S), $N = S + 1$, and $a_n = T_0$; here the n-th component, called "others" in table 3, comprises all other than significant components plus SiO_2. Hence,

$$x_n = 1 - \sum_{i=1}^{S} x_i \quad (13)$$

Table 3 lists the a_i coefficients for the log(η (Pas)) = = 1.5 isokom.

In this contribution, the values of A_i and B_i coefficients were obtained by fitting equation (6) to viscosity versus temperature and composition data for individual glass types (local models) as well as for all commercial glasses tested (a global model). Generally, global models cover large composition regions whereas local models are developed for compositional neighborhoods of base glasses formulated for various applications and production technologies.

Table 3. Component coefficients for η = 31.6 Pas isokom in °C (Fluegel et al., Chapter 9 in [6]).

	F+C	E	TV	FW
Al_2O_3	2183			
B_2O_3		-15		-306
BaO			700	
CaO	237	-82	371	260
F			-3140	
Fe_2O_3	322			
K_2O	398		300	-427
Li_2O	-4707	1837	-3463	
MgO	698	494		1287
Na_2O	-533	93	-912	-670
PbO			727	
SrO			535	
TiO_2	-295		-3483	
Others	1811	1837	1865	1848

The F+C column lists coefficients for float glass (F) plus container glass (C). Component coefficients for η = 31.6 Pas isokom are not reported for low-expansion (LE) glasses."Others" are all remaining components including SiO_2 [see equation (13)].

Table 2. Component coefficients for isokoms.

η (Pas)	3.16×10^1	3.98×10^6	1.00×10^{12}	η (Pas)	3.16×10^1	3.98×10^6	1.00×10^{12}
		T_0 (K)				T_{ij}	
	1816.4	876.7	618.4	$Al_2O_3\times B_2O_3$		-0.625	-0.626
		T_i		$Al_2O_3\times MgO$	-0.526	-0.911	
Al_2O_3	4.35	15.48	11.24	$Al_2O_3\times Na_2O$	0.761	-0.686	
B_2O_3	-13.49	-3.16	-3.10	$B_2O_3\times K_2O$			0.585
BaO	-22.26	-4.16		$B_2O_3\times Na_2O$	-0.536	0.156	0.573
CaO	-18.00	-2.77	1.05	$B_2O_3\times CaO$	-0.225	-0.117	
F	-14.73	-6.14	-9.33	CaO×F	1.017		
FeOx	-15.33	-6.79		$CaO\times K_2O$		0.334	0.468
K_2O	-19.21	-11.90	-11.94	$CaO\times Na_2O$	0.215	0.207	0.157
Li_2O	-29.14	-16.81	-21.06	$F\times K_2O$		-0.565	
MgO	-5.99	4.02	-1.54	$K_2O\times MgO$	0.788		
Na_2O	-25.10	-11.27	-7.30	$MgO\times Na_2O$		-0.174	
PbO	-23.22	-8.62	-4.61			T_{ijk}	
SrO	-20.09	-3.01	2.25	$Al_2O_3\times B_2O_3\times Na_2O$			-0.0449
ZnO	-9.42	-1.67		$Al_2O_3\times CaO\times Na_2O$			-0.0285
ZrO_2		9.51	9.03	$Al_2O_3\times MgO\times Na_2O$		0.0732	
				$B_2O_3\times CaO\times Na_2O$			-0.0111
				$CaO\times MgO\times Na_2O$	-0.0211	-0.0282	

RESULTS

Viscosity data for three (LE 16, FW 18, and E 20) out of 150 glasses originally designed were not available because these glasses were never fabricated. With two exceptions, Li_2O and K_2O, only mass fractions of components with ≥1 mass% were selected for fitting. Although fluorine is a minor component that strongly impacts viscosity, its mass fraction was not included as a variable because including it did not improve the outcome. To obtain A_i and B_i values, equation (6) was fitted to data. The compositions were not renormalized (to make the sum of mass fractions equal to 1) when minor components were excluded from calculations. Of the 147 glasses for which viscosity data were available, three were eliminated as outliers (E 3, F 9, and TV 8). Several individual data points were also removed as outliers. The outliers were selected based on local models as glasses with unusually high values of $\Delta^2 = [\ln(\eta_m/\eta_c)]^2$, where the subscript *m* stands for measured and *c* for calculated values (using local models with outliers removed). In the extreme case of E-glasses, the difference between Δ^2 values for outliers was substantially higher than Δ^2 values for regular data ($\Delta^2 \geq 4.5$ for outliers and $\Delta^2 \leq 0.28$ for all other data). For other glass groups, these differences were lower: 3.6 and 0.57 for LE, 0.77 and 0.31 for FW, 0.50 and 0.39 for FW, 0.45 and 0.13 for F; no outliers were identified in C glasses.

Table 4 lists A_i and B_i values of the global model obtained by fitting equation (6) to all data except outliers. Table 5 summarizes the values of A_i, B_i, and $\ln(\eta_{i,1500°C})$ for individual types of glasses (local models).

Table 4. Component coefficients for viscosity in Pas, global model.

	A_i	$B_i 10^3$ K	$\ln(\eta_i$(Pas)) at 1500°C
SiO_2	-6.25	24.14	7.37
TiO_2	-26.72	28.15	-10.84
ZrO_2	-8.41	22.88	4.49
Al_2O_3	12.68	-4.66	10.06
Fe_2O_3	19.39	-35.05	-0.37
B_2O_3	0.45	-14.74	-7.86
MgO	-41.91	60.26	-7.93
CaO	-53.10	66.80	-15.43
SrO	-18.19	20.84	-6.44
BaO	-15.99	19.51	-4.99
PbO	-13.39	11.89	-6.68
ZnO	-39.25	67.15	-1.38
Li_2O	-80.42	50.11	-52.16
Na_2O	-13.02	-2.12	-14.22
K_2O	-27.10	30.05	-10.15
R^2	0.984		
R^2adj	0.983		

Table 5. Component coefficients for viscosity (in Pas), local models.

	A_i					
	E	F	LE	TV	FW	C
SiO_2	-5.65	-6.52	-9.64	-11.36	-17.97	-8.43
TiO_2	38.62	-59.51				
ZrO_2				-17.19		
Al_2O_3	-28.47	9.72	67.39	29.72	4.13	-6.78
Fe_2O_3		-37.04				
B_2O_3	10.17		1.15		-11.48	
MgO	-49.06	-48.40		-24.32	-31.82	-16.66
CaO	-34.53	-48.11	-57.84	-12.15	-66.91	-16.62
SrO				-21.97		
BaO			-53.64	-15.36		
PbO				-41.12		
ZnO				-28.75		
Li_2O						-98.08
Na_2O	0.91	-7.51	-44.15	25.28	45.54	-21.40
K_2O	-78.02	-16.67	-31.83	-33.79	-8.52	-7.84

	10^{-3} B_i (K)					
	E	F	LE	TV	FW	C
SiO_2	27.62	23.25	31.01	31.28	41.64	26.16
TiO_2	-69.55	90.75				
ZrO_2				39.28		
Al_2O_3	47.71	2.45	-69.48	-26.18	8.73	34.93
Fe_2O_3		60.30				
B_2O_3	-28.43		-11.78		-2.20	
MgO	65.01	69.96		49.27	54.73	20.68
CaO	34.30	63.10	80.83	5.67	94.41	14.97
SrO				26.59		
BaO			84.06	19.30		
PbO				54.34		
ZnO				49.55		
Li_2O						77.22
Na_2O	-22.82	-8.16	11.39	-72.05	-91.92	12.97
K_2O	112.93	18.44	23.14	50.04	-0.93	11.52

	$\ln(\eta_{i1500°C}$ (Pas))					
	E	F	LE	TV	FW	C
SiO_2	9.93	6.60	7.85	6.28	5.51	6.32
TiO_2	-0.61	-8.33				
ZrO_2				4.97		
Al_2O_3	-1.56	11.11	28.20	14.95	9.06	12.92
Fe_2O_3		-3.03				
B_2O_3	-5.86		-5.50		-12.72	
MgO	-12.39	-8.94		3.47	-0.95	-5.00
CaO	-15.18	-12.52	-12.25	-8.95	-13.66	-8.17
SrO				-6.97		
BaO			-6.23	-4.47		
PbO				-10.47		
ZnO				-0.80		
Li_2O						-54.53
Na_2O	-11.97	-12.11	-37.73	-15.36	-6.31	-14.08
K_2O	-14.33	-6.27	-18.78	-5.56	-9.04	-1.34

DISCUSSION

Figure 3 compares calculated versus measured values for viscosity, and table 6 lists the values of R^2 and R^2_{adj} that express the fraction of variability accounted for by the model (R^2_{adj} is adjusted for the number of parameters used in fitting the model). As expected, both figure 3 and table 6 show that the individual fits predict viscosity values better than the overall fit. The difference between viscosity predicted by the local models and the global model is the smallest for float glass (F) and the largest for low-expansion glass (LE). As figure 2 shows, float glass has the smallest variability of data, and low-expansion glass is the most difficult to melt. Models for all individual glass types have high R^2 values ranging from 0.97 for TV glasses to 0.99 for float glasses. The global model represents viscosity data as a whole with a good R^2 value of 0.98. However, when the global model is applied to individual glass types, R^2 values vary from 0.92 to 0.98, except for low-expansion glasses for which the fit is rather poor (R^2 = 0.75).

Table 6. R^2 values for viscosity models.

	E	F	LE	TV	FW	C	All
R^2_{ind}	0.982	0.989	0.967	0.965	0.967	0.983	
R^2_{all}	0.939	0.981	0.748	0.923	0.940	0.962	0.984
$R^2_{adj,ind}$	0.979	0.987	0.961	0.955	0.961	0.981	
$R^2_{adj,all}$	0.926	0.978	0.700	0.901	0.930	0.957	0.983

As figure 3 and table 6 indicate, local models are generally more accurate than the global model within the composition regions of their databases (listed in table 1). The global model is recommended for compositions within the overall composition region that are not covered by any of the local models. However, for high-viscosity-high-temperature glasses (the LE type), the global model may perform rather poorly.

The effect of composition change on viscosity can be expressed as the change in viscosity, $\Delta\eta_j$, caused by replacing a mass fraction of silica ($-\Delta x$) with the same mass fraction (Δx) of j-th oxide. By equation (7),

$$\Delta\eta_j = \eta_0 \{\exp [\Delta x (Z_j - Z_{SiO_2})] - 1\} \qquad (14)$$

where η_0 is the melt viscosity before the fraction of silica was replaced with the same mass of j-th oxide, and $Z_j = \ln[\eta_j(T)]$ is the partial specific logarithmic viscosity at temperature T (shown in tables 3 and 4 for T = = 1500°C). By equation (14), the j-th component tends to increase the melt viscosity when $\Delta\eta_j > 0$ at 1500°C. Calculations were performed for $Z_j = \ln(\eta_{i,1500°C}$ (Pas)), Δx = 0.02 (2 mass% replacement) and η_0 = 10 Pas. Figures 4 and 5 display the results for several major glass components. In figure 4, the $\Delta\eta_j$ values are based on Z_j values from the global model. Figure 5 compares $\Delta\eta_j$ values based on local models with those from the global model. As expected, B_2O_3, Na_2O, K_2O, MgO, and CaO decrease glass viscosity when replacing SiO_2 whereas Al_2O_3 tends to increase viscosity except for the low-alkali E-glass. Note that in the high–silica–high––boria LE glass, Al_2O_3 and Na_2O have a significantly higher impact on viscosity than in any other glass tested.

In glass technology, it is often important to know how rapidly viscosity changes with changing temperature and how the rate of change is affected by glass composition. By equation (2),

$$\frac{\partial \ln\eta}{\partial T} = -\frac{B}{T^2} \qquad (15)$$

Since viscosity decreases as temperature increases, B is always positive, and the higher the B at a given temperature, the steeper the slope. Consequently, as molten glass gets cooler, its viscosity increases less with decreasing temperature when the B value is small; such a glass is called a "long" glass because it takes a longer time to reach a high viscosity at a given rate of cooling. This is illustrated in figure 6, which plots the temperature increase (starting from 1500°C) associated with a 10-times increase in melt viscosity as a function of B.

The average B value for glasses tested in this study is B_a = 2.38 10^4 K. With a glass "length" component effect defined as $L_i = B_i - B_a$, components with $L_i > 0$ tend to "lengthen" the glass and components with $L_i < 0$ tend to "shorten" it. Figure 7 compares the effects of several components on the melt "length" at glass processing temperatures. This picture will change at glass-forming temperatures because the Arrhenius relationship no longer represents the melt viscosity-temperature relationship for commercial glasses below 1000°C.

The log(η (Pas)) = 1.5 (η = 31.6 (Pas)) isokoms were obtained from equation (9) with the coefficient values listed in table 4. To compare the results of calculations with experimental data, the temperature, $T_{31.6}$, at which η = 31.6 Pas, was obtained by fitting equation (2) to data for each glass. Figure 8 shows the result together with a similar plot in which the Fuegel et al. [7] model is compared with $T_{31.6}$ values obtained from experimental data. The vertical lines in figure 8 indicate the maximum temperature of the viscosity measurement, beyond which all values are extrapolated. As figure 9 shows, both models predict similar $T_{31.6}$ values for T < 1400°C. For higher temperatures, the Fluegel et al. [7] model seems to underpredict the isokoms, provided that extrapolated data can be trusted. However, high temperatures are outside the application limits of the Fluegel et al. model; most extrapolated temperature values from data obtained at lower temperatures were excluded from the model database [7].

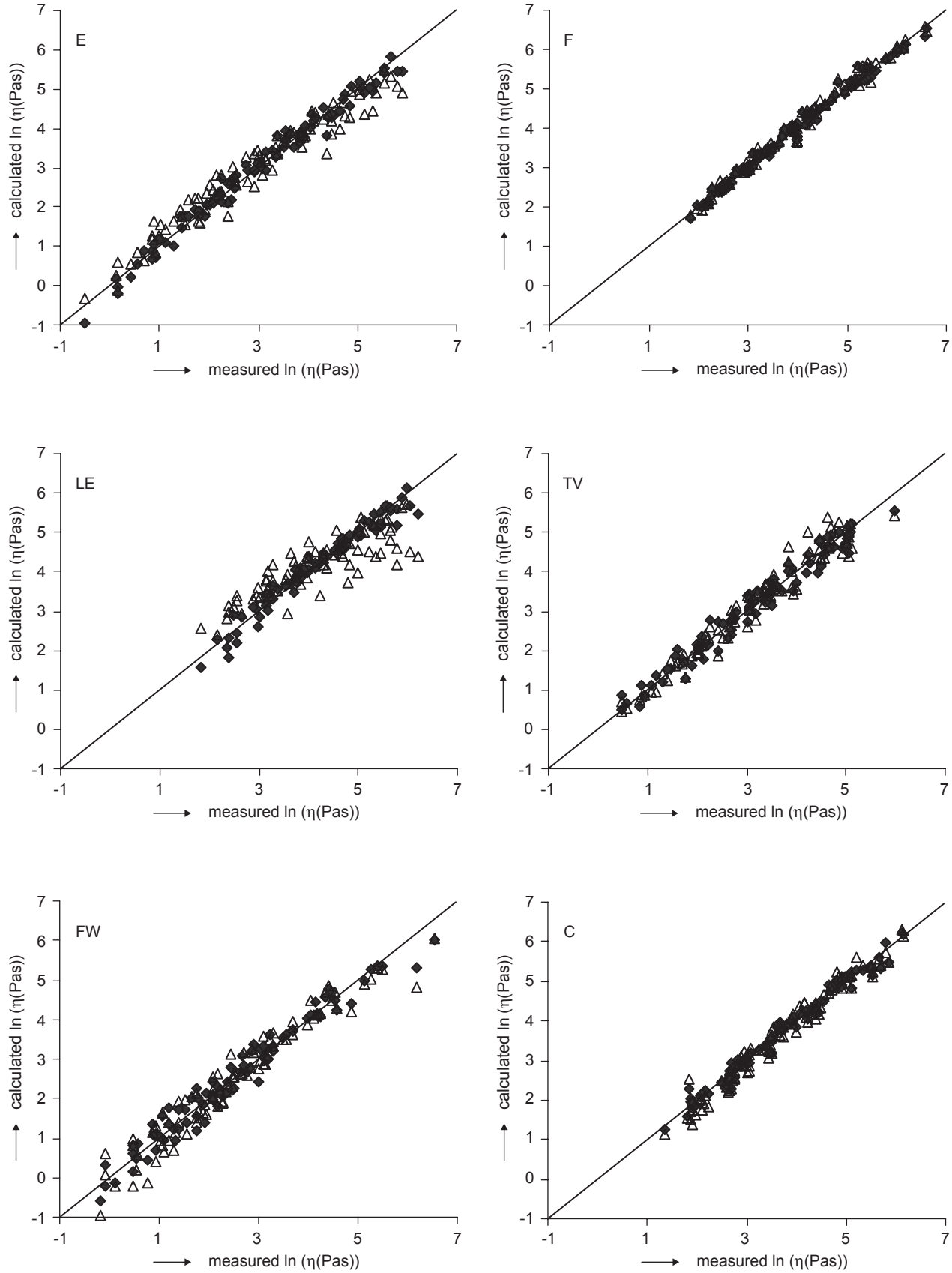

Figure 3. Calculated versus measured values for viscosity; solid points represent local models, and hollow points stand for the global model applied to individual glass types.

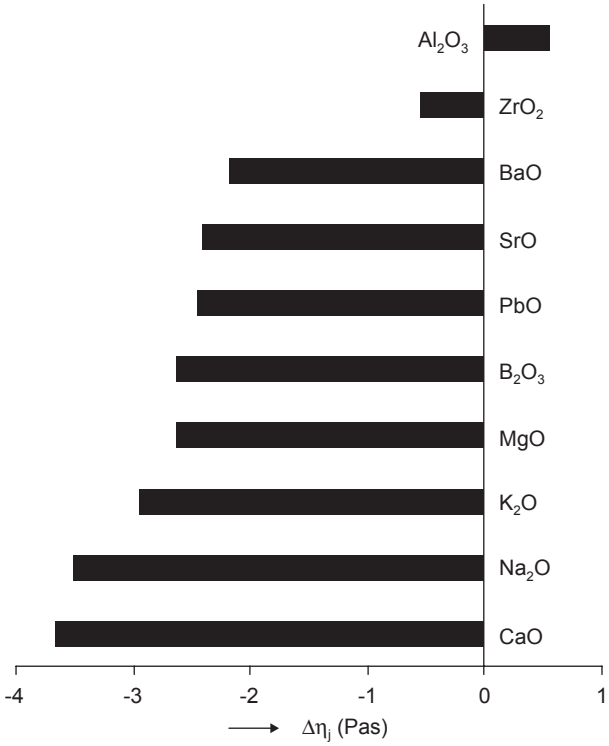

Figure 4. Effect of replacing 2 mass% SiO_2 with another oxide on melt viscosity at 1500°C.

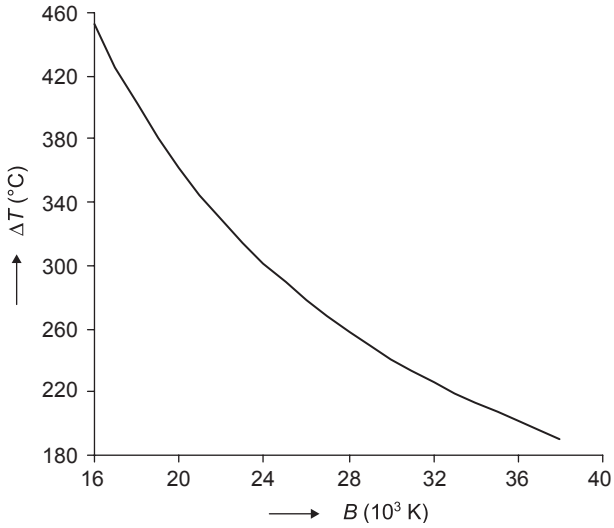

Figure 6. Effect of B on the temperature decrease (ΔT) from 1500°C that results in a 10 times increase in melt viscosity.

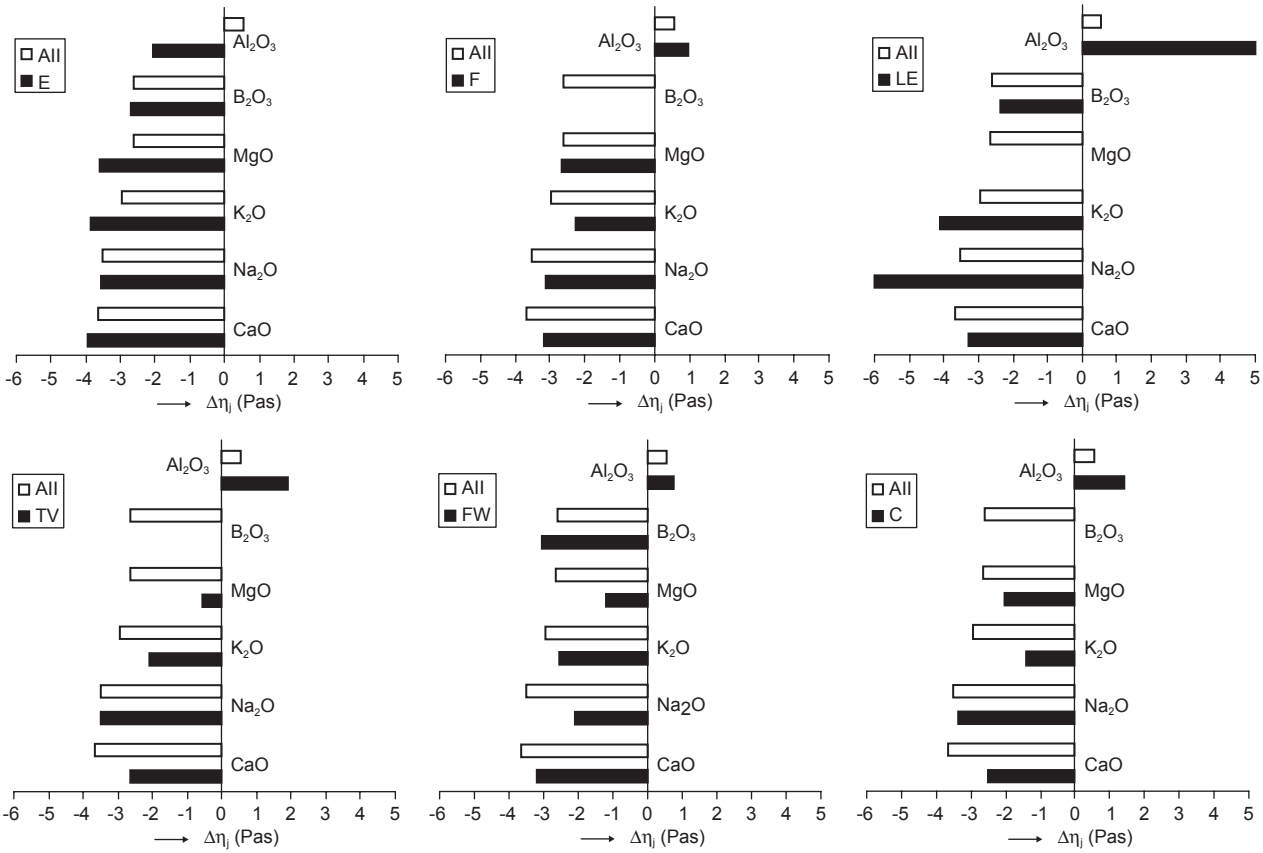

Figure 5. Effect of replacing 2 mass% SiO_2 with another oxide on melt viscosity at 1500°C: comparison of individual glass types with the full set of data.

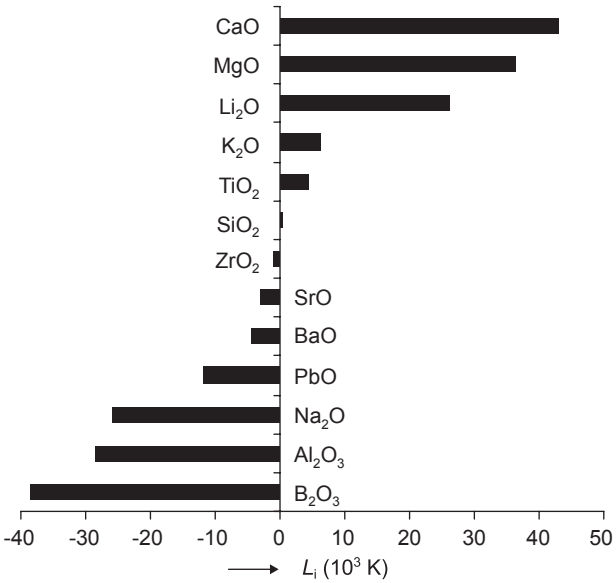

Figure 7. Effect of glass components on melt "length".

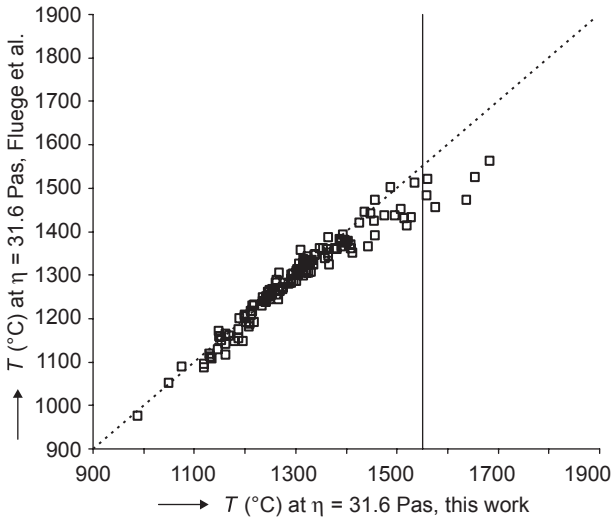

Figure 9. $T_{31.6\ Pas}$ isokom obtained using the nonlinear model by Fuegel et al. [7] versus the global Arrhenius model (table 4).

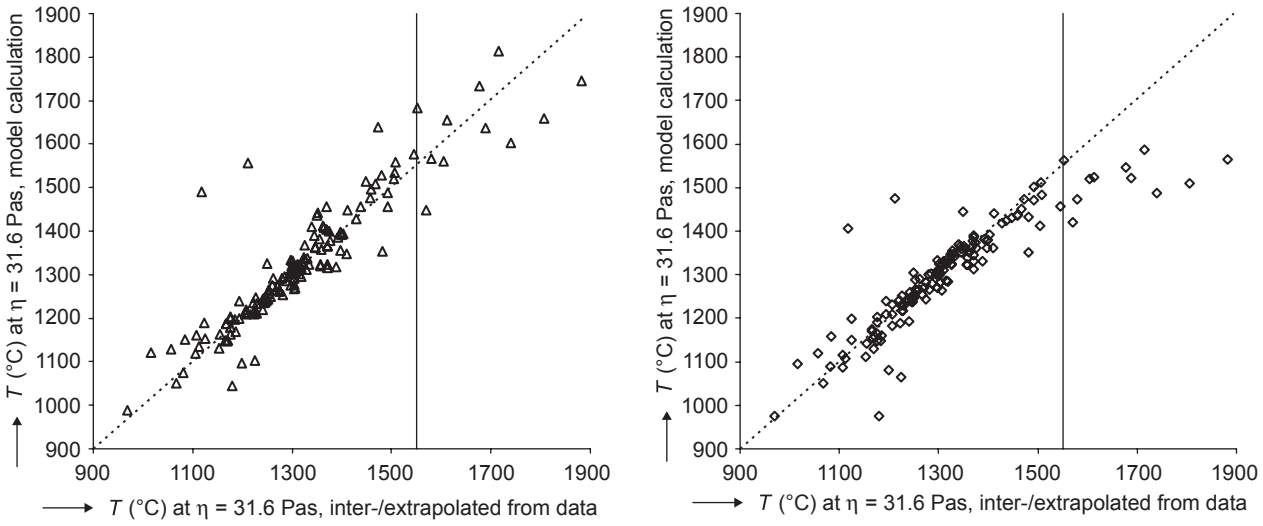

Figure 8. $T_{31.6\ Pas}$ isokom, model calculation versus values obtained for experimental data; left: Arrhenius model with 30 coefficients listed in table 4; right: Fluegel et al. [7] model, equation (10), with 22 coefficients listed in table 2.

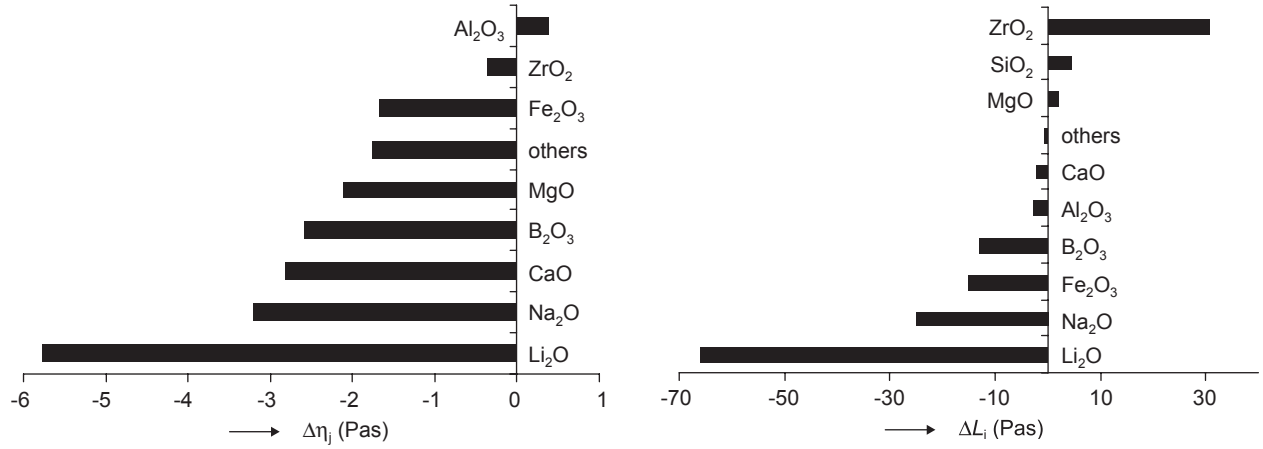

Figure 10. Effect of components on high-level waste glass viscosity (left) and "length" (right).

Finally, it may be of interest to compare commercial and waste glasses with respect to the effects of glass components on their viscosity. Table 7 lists the composition region and the Arrhenius coefficients for the viscosity of these glasses [3]. Viscosity data for the waste glasses were measured within 950°C and 1250°C, and viscosity values ranged from 0.4 to 90 Pas at 1150°C. Figure 10 shows the values of $\Delta\eta_j$ (Δx = 0.02, η_0 = = 10 Pas, and T = 1150°C) and L_i. A comparison of figures 4 and 10 reveals that the impact of replacing SiO_2 with an equal mass of another component is very similar in commercial and waste glasses. However, the impacts of glass components on melt "length" are different, indicating that the differences in composition regions and temperature ranges significantly influence the secondary properties (such as the temperature derivative of viscosity) of melts.

Table 7. Composition region and viscosity coefficients for high-level waste glasses [3].

	Mass fraction ranges		Viscosity coefficients	
	x_{min}	x_{max}	A_i	$10^{-3}B_i$ (K)
SiO_2	0.42	0.57	-11.1	28.5
B_2O_3	0.05	0.20	-13.7	10.9
Na_2O	0.05	0.20	-9.6	-1.2
Li_2O	0.01	0.07	-4.5	-42.3
CaO	0.00	0.10	-22.8	21.5
MgO	0.00	0.08	-21.1	25.8
Fe_2O_3	0.005	0.15	-6.4	8.8
Al_2O_3	0.00	0.17	-4.1	21.2
ZrO_2	0.00	0.13	-31.3	54.6
Others	0.01	0.10	-17.0	23.0

CONCLUSION

For the processing temperature range for common commercial glasses (1100°C to 1550°C), the Arrhenius relationship represents the viscosity-temperature relationship reasonably well; the R^2 ranges from 0.97 to 0.99 for six local models developed for individual glass types (E glass, float glass, low-expansion-borosilicate glass, TV panel glass, fiberglass wool, and container glass) and 0.98 for the global model covering the whole composition region of commercial glasses containing 42 to 84 mass% SiO_2. The models adequately represent the viscosity-temperature relationship of glass at $\eta < 10^3$ Pas, or, more accurately, 5 to 400 Pas. The global Arrhenius model was found in good agreement with a nonlinear model developed by Fluegel et al. [7]. The component effects were found similar to those previously established for high-level waste glasses.

References

1. Scholze H.: *Glass*, Springer, New York 1990.
2. Bansal N. P., Doremus R. H.: *Handbook of Glass Properties*, Academic Press, Orlando 1986.
3. Hrma P., Piepel G. F., Redgate P. E., Smith D. E., Schweiger M. J., Vienna J. D., Kim D-S.: Ceramic Transactions *61*, 505 (1995).
4. Hrma P.: Ceramic Transactions *87*, 245 (1998).
5. Piepel G. F., Hrma P., Vienna J. D.: *Glass Chemistry Development Strategy For Hanford High Level Waste (HLW)*, in *Science and Technology for Disposal of Radioactive Tank Wastes*, pp. 393-402, Plenum Press, New York 1998.
6. Seward III T. P., Vascott T. (Editors): *High temperature glass melt property database for process modeling*, American Ceramic Society, Westerville, Ohio 2005.
7. Fluegel A., Varshneya A. K., Earl D. A., Seward T. P., Oksoy D.: *Improved Composition-Property Relations in Silicate Glasses, Part I: Viscosity*, Ceramic Transaction [in print].

VYSOKOTEPLOTNÍ VISKOZITA PRŮMYSLOVÝCH SKEL

PAVEL HRMA

Pacific Northwest National Laboratory
Richland, WA 99352, United States of America

Závislost viskozity skelných tavenin v oblasti tavicích teplot byla aproximována lineárními modely na bázi Arrheniovy rovnice pro šest typů průmyslových skel: borosilikátová skla s nízkým koeficientem tepelné roztažnosti, E skla, skelná vata, skla pro televizní obrazovky, obalová skla, a skla float. Modely reprezentují závislost viskozity na teplotě a složení jak pro jednotlivé typy skel (lokální modely) tak pro celkovou oblast složení průmyslových skel (globální model). Modelové koeficienty byly optimalizovány s použitím viskozitních dat změřených rotačním viskozimetrem v rozmezí 900-1550°C, ve kterém viskozita nabývala hodnot 1-750 Pas, pro 15 složek: SiO_2, TiO_2, ZrO_2, Al_2O_3, Fe_2O_3, B_2O_3, MgO, CaO, SrO, BaO, PbO, ZnO, Li_2O, Na_2O a K_2O. R^2 nabyla hodnoty 0.98 pro globální model a 0.97 až 0.99 pro šest lokálních modelů. Modely lze doporučit pro průmyslová skla s obsahem 42-84 % SiO_2 k odhadu viskozit nebo teplot pro danou hodnotu viskozity skelných tavenin v rozmezí teplot 1100-1550°C a viskozit 5-400 Pas.